J|A|C|S
ARTICLES
Published on Web 05/27/2006

Sol−Gel Assembly of CdSe Nanoparticles to Form Porous Aerogel Networks

Indika U. Arachchige and Stephanie L. Brock*

Contribution from the Department of Chemistry, Wayne State University, Detroit, Michigan 48202

Received March 6, 2006; E-mail: sbrock@chem.wayne.edu

Abstract: A detailed study of CdSe aerogels prepared by oxidative aggregation of primary nanoparticles (prepared at room temperature and high temperature conditions, >250 °C), followed by CO_2 supercritical drying, is described. The resultant materials are mesoporous, with an interconnected network of colloidal nanoparticles, and exhibit BET surface areas up to 224 m^2/g and BJH average pore diameters in the range of 16−32 nm. Powder X-ray diffraction studies indicate that these materials retain the crystal structure of the primary nanoparticles, with a slight increase in primary particle size upon gelation and aerogel formation. Optical band gap measurements and photoluminescence studies show that the as-prepared aerogels retain the quantum-confined optical properties of the nanoparticle building blocks despite being connected into a 3-D network. The specific optical characteristics of the aerogel can be further modified by surface ligand exchange at the wet-gel stage, without destroying the gel network.

Introduction

Aerogels are a unique class of porous inorganic polymers with low densities, large open pores, and high inner surface areas. They consist of an interconnected network of nanometer scale solid building blocks, which result in both micropores (<2 nm) and mesopores (2−50 nm) throughout the material.[1,2] Typically, the solid content of an aerogel network is 1−15 vol %, resulting in densities as low as 3 times that of air. These features of aerogels result in interesting physical properties as well as a wide variety of actual and potential applications as catalysts, sensors, thermal insulators, cosmic dust collectors, and novel electrochemical device components.[1,2] So far, a great deal of research has been conducted on aerogels based on single and mixed metal oxides, with the traditional SiO_2, Al_2O_3, and TiO_2 aerogels among the most widely studied systems. Hence, aerogels have been largely limited to either insulators or wide band gap semiconductors for many years. However, during the last two decades, scientists have begun to produce aerogels based on conductive materials for applications as batteries, capacitors, and fuel cells.[3] In these systems, conductivity is achieved by assembling the aerogel network from native conducting oxides (V_2O_5,[4−6] MnO_2[7,8]) or by "wiring" a metallic component through an insulating aerogel network (SiO_2/RuO_2[9]).

In principle, an extensive range of aerogel chemical and physical properties can be achieved if the framework can be assembled from components other than oxides, a premise that is largely unexplored. Specifically, the synthesis of aerogel networks based on 12−16 semiconductors is expected to lead to novel properties due to the marriage of the quantum-confined electro-optical properties inherent to the nanoparticle building blocks,[10,11] with the high surface area and porosity of the aerogel network. Among the 12−16 semiconductor quantum dots, CdSe materials have gained considerable attention from the scientific community due to their relative ease of synthesis, the ability to tune the optical absorption throughout much of the visible spectrum, and the sharpness and high intensity of band-edge luminescence. Accordingly, there have been numerous reports on the synthesis and characterization of CdSe nanomaterials that demonstrate excellent control of size, shape, and polydispersity, as well as investigations of CdSe nanomaterials for applications in nonlinear optical devices,[12] biological labeling and diagnostics,[13] electro-luminescent[14,15] and photovoltaic devices,[16−18] and

(1) Rolison, D. R.; Dunn, B. *J. Mater. Chem.* **2001**, *11*, 963−980.
(2) Hüsing, N.; Schubert, U. *Angew. Chem., Int. Ed.* **1998**, *37*, 22−45.
(3) Merzbacher, C. I.; Baker, J. G.; Long, J. W.; Rolison, D. R. *Nanostruct. Mater.* **1999**, *12*, 551−558.
(4) Le, D. B.; Passerini, S.; Coustier, F.; Guo, J.; Soderstrom, T.; Owens, B. B.; Smyrl, W. H. *Chem. Mater.* **1998**, *10*, 682−684.
(5) Le, D. B.; Passerini, S.; Tipton, A. L.; Owens, B. B.; Smyrl, W. H. *J. Electrochem. Soc.* **1995**, *142*, L102.
(6) Dong, W.; Rolison, D. R.; Dunn, B. *Electrochem. Solid State Lett.* **2000**, *3*, 457.
(7) Long, J. W.; Stroud, R. M.; Rolison, D. R. *J. Non-Cryst. Solids* **2001**, *285*, 288−294.
(8) Long, J. W.; Young, A. L.; Rolision, D. R. *J. Electrochem. Soc.* **2003**, *150*, A1161−A1165.
(9) Ryan, J. V.; Berry, A. D.; Anderson, M. L.; Long, J. W.; Stroud, R. M.; Cepak, V. M.; Browning, V. M.; Rolision, D. R.; Merzbacher, C. I. *Nature* **2000**, *406*, 169−172.
(10) Wang, Y.; Herron, N. *J. Phys. Chem.* **1991**, *95*, 525−532.
(11) Alivisatos, A. P. *Science* **1996**, *271*, 933−937.
(12) Amore, F. D.; Pietralunga, S. M.; Lorusso, P.; Martinelli, M.; Zappettini, A.; Dal Bo, E.; Tassone, F.; Tognini, P.; Travagnin, M. *Phys. Status Solidi C* **2004**, *1*, 1001−1004.
(13) Michalet, X.; Pinaud, F. F.; Bentolila, L. A.; Tsay, J. M.; Doose, S.; Li, J. J.; Sundaresan, G.; Wu, A. M.; Gambhir, S. S.; Weiss, S. *Science* **2005**, *307*, 538−544.
(14) Colvin, V. L.; Schlamp, M. C.; Alivisatos, A. P. *Nature* **1994**, *370*, 354−357.
(15) Dabbousi, B. O.; Bawendi, M. G.; Onitsuka, O.; Rubner, M. F. *Appl. Phys. Lett.* **1995**, *66*, 1316−1318.
(16) Huynh, W. U.; Dittmer, J. J.; Alivisatos, A. P. *Science* **2002**, *295*, 2425−2427.
(17) Liu, J.; Tanaka, T.; Sivula, K.; Alivisatos, A. P.; Fréchet, J. M. J. *J. Am. Chem. Soc.* **2004**, *126*, 6550−6551.
(18) Sun, B.; Marx, E.; Greenham, N. C. *Nano. Lett.* **2003**, *3*, 961−963.

10.1021/ja061561e CCC: $33.50

Table 1. Comparison of Elemental Compositions, Optical Chromophore, Crystallite and Primary Particle Sizes of Precursor CdSe Nanoparticles Prepared by Inverse Micellar and High Temperature Routes and the Resultant As-Prepared Aerogels; BET Surface Areas with Silica Equivalence Values (calculated on a per mole basis), BJH Adsorption Average Pore Diameters, and Cumulative Pore Volumes for Aerogels Degassed at 100 °C

Material	Thiolate-Coated CdSe Nanoparticles		CdSe Aerogel[c]	
synthetic method	inverse micellar[d]	high temperature[e]	inverse micellar[d]	high temperature[e]
absorption band onset	515 nm	550 nm	557 nm	595 nm
optical chromophore size[a]	4.4 nm	5.0 nm	5.1 nm[a]	5.9 nm[a]
crystallite size[b] (PXRD)	2.5 nm	2.8 nm	2.7 nm	3.0 nm
primary particle size (TEM)	2.8 ± 0.4 nm	3.0 ± 0.5 nm	3.8 ± 0.5 nm	4.0 ± 0.5 nm
elemental composition in atomic percentages (SEM/EDS)	Cd 40.2% Se 39.6% S 20.2%	Cd 38.9% Se 37.7% S 19.3% P 4.1%	Cd 46.2% Se 43.6% S 10.2%	Cd 42.1% Se 40.5% S 13.5% P 3.9%
BET surface area[f]			128−161 m^2/g	106−124 m^2/g
silica equivalence BET surface area[f,g]			408−513 m^2/g	338−395 m^2/g
BJH adsorption average pore diameter[f]			16−29 nm	23−28 nm
BJH adsorption cumulative pore volume[f]			0.53−0.98 cm^3/g	0.63−0.72 cm^3/g

[a] Particle sizes were calculated using the absorption onset and mass approximation model. [b] Crystallite sizes were calculated by employing the Scherrer formula[29] to the (111) peak of inverse micellar prepared particles (cubic) or the (110) peak of high temperature prepared nanoparticles (hexagonal). [c] Tetranitromethane was used as the oxidant in gel formation. [d] Primary nanoparticles are capped with 4-fluorobenzenethiol before the gelation. [e] Primary nanoparticles are capped with 11-mercaptoundecanoic acid before the gelation. [f] Range of values represents the spread from three independently prepared samples. [g] Values were computed by converting the BET surface area for 1 mol of CdSe aerogel into that for a mol of silica using the respective formula weights.

sensors.[19−21] One remaining challenge for application of CdSe nanoparticles in functional solid-state devices is the development of methods to assemble nanoparticles together while retaining their unique optical and electronic properties. Gelation and aerogel formation represents a simple way to assemble nanoparticles in three dimensions since aerogels can be represented as a fractal network of aggregated nanoparticles. Such a material would be uniquely poised for applications that cannot be optimally addressed by discrete nanoparticles or bulk materials, including high surface area self-supported sensors and photocatalysts, as well as components for photovoltaic devices.

In 1997, Gacoin reported the synthesis of transparent CdS gels from concentrated sols of CdS nanoparticles.[22,23] In these syntheses, Gacoin used an inverse micelle route to prepare CdS nanoparticles that are complexed on the surface with 4-fluorophenylthiolate. Controlled oxidation of these surface thiolate groups using H_2O_2 resulted in CdS gels. Recently, our group has reported the synthesis of CdS aerogels using the sol−gel method developed by Gacoin, followed by supercritical fluid extraction to maintain the wet-gel morphology during drying.[24] Additionally, we have shown that this method can be extended to CdSe, ZnS, and PbS, as well as CdSe nanoparticles prepared by high temperature routes that are surface complexed with 11-mercaptoundecanoic acid.[25] The pore size of these materials is appropriate for molecular transport or infiltration of secondary components, and the quantum confinement in these materials can be further tuned by adjusting the density of the framework.[26] In the present work, a detailed comparison of the properties of CdSe aerogels prepared from nanoparticles synthesized at room temperature and at high temperature (>250 °C) is conducted. The versatility of the nanoparticle assembly approach is further demonstrated through a study of different gelation agents, capping groups, and other synthetic parameters. The structural, optical, electronic, and surface properties of the resultant aerogels can be adjusted by varying the characteristics of the nanoparticle building blocks and/or by surface modification at the wet-gel stage.

Results

Nanoparticle Synthesis, Gelation, and Aerogel Formation. CdSe nanoparticles were prepared using standard room temperature inverse micellar strategies and a high temperature synthetic route employing highly coordinating surfactant ligands. These nanoparticles were complexed with the thiolate ligands, 4-fluorobenzenethiol (inverse micellar route) or 11-mercaptoundecanoic acid (high temperature route), and dispersed in acetone or methanol, respectively, to make orange−red colored CdSe sols. Absorption onset values and the average particle sizes calculated based on the optical absorption and powder X-ray diffraction (PXRD) data are shown in Table 1.

Controlled oxidation of the surface-bound thiolate groups was achieved by using either a chemical oxidizing agent (tetranitromethane or H_2O_2) or photooxidation[27] using ambient fluorescent lighting. Photooxidation is a slow process, leading to gel formation within 7−10 days for high temperature synthesized CdSe nanoparticles and within 4−5 weeks for CdSe nanoparticles prepared by the inverse micellar route. On the other hand, the use of a chemical oxidant (tetranitromethane or H_2O_2) leads to gelation within 1−2 h. The resulting orange−red colored wet gels were aged for 10−14 days under ambient conditions to form opaque monolithic wet gels, and the byproducts of the oxidation (disulfides and sulfonates[28]) were removed by exchanging the solvent of the wet gel 6−8 times with acetone over 2−3 days. In some cases, the wet gels were exchanged several times with pyridine prior to the acetone

(19) Ivanisevic, A.; Reynolds, M. F.; Burstyn, J. N.; Ellis, A. B. *J. Am. Chem. Soc.* **2000**, *122*, 3731−3738.
(20) Nazzal, A. Y.; Lianhua, Q.; Peng, X.; Xiao, M. *Nano. Lett.* **2003**, *3*, 819−822.
(21) Meeker, K.; Ellis, A. B. *J. Phys. Chem. B* **1999**, *103*, 995−1001.
(22) Gacoin, T.; Malier, L.; Boilot, J.-P. *J. Mater. Chem.* **1997**, *7*, 859−860.
(23) Gacoin, T.; Malier, L.; Boilot, J.-P. *Chem. Mater.* **1997**, *9*, 1502−1504.
(24) Mohanan, J. L.; Brock, S. L. *J. Non-Cryst. Solids* **2004**, *350*, 1−8.
(25) Mohanan, J. L.; Arachchige, I. U.; Brock, S. L. *Science* **2005**, *307*, 397−400.
(26) Arachchige, I. U.; Mohanan, J. L.; Brock, S. L. *Chem. Mater.* **2005**, *17*, 6644−6650.
(27) Aldana, J.; Wang, Y. A.; Peng, X. *J. Am. Chem. Soc.* **2001**, *123*, 8844−8850.
(28) Gacoin, T.; Lahlil, K.; Larregaray, P.; Boilot, J.-P. *J. Phys. Chem. B* **2001**, *105*, 10228−10235.

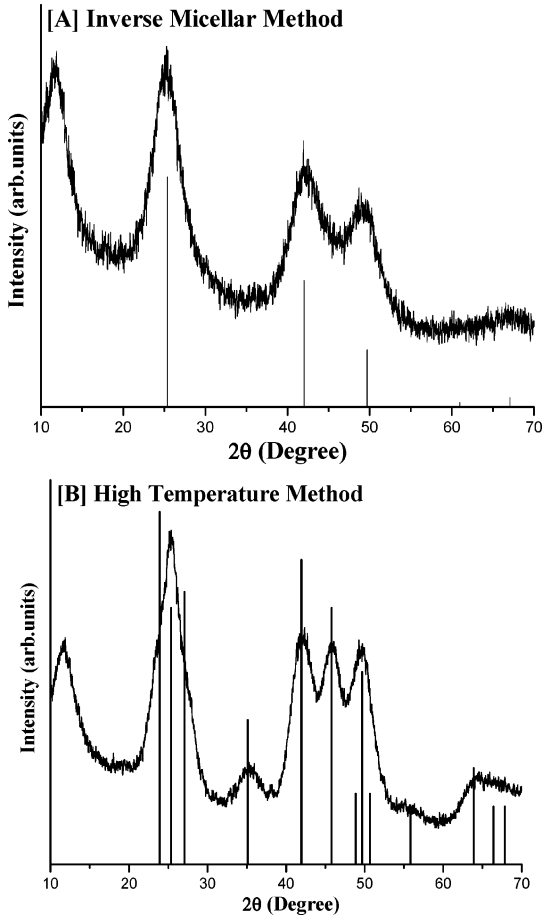

Figure 1. PXRD patterns of CdSe aerogels prepared from (A) inverse micellar synthesized and (B) high temperature synthesized nanoparticles. The ICDD-PDF overlays of cubic CdSe (PDF # 19-0191) and hexagonal CdSe (PDF # 08-0459) are shown as vertical lines in (A) and (B), respectively. The prominent peak at ~12° is an amorphous signal due to the grease employed to affix the sample to the holder. The small peak at ~38° in (B) can be attributed to a minor degree of CdO formation from surface oxidation.

exchanges in an effort to remove residual thiolate. The acetone-exchanged wet gels were dried using supercritical CO_2 to form CdSe aerogels. The resultant CdSe aerogels were orange in color and showed a 5−10% apparent volume loss when compared to precursor wet gels.

Effect of Nanoparticle Synthetic Route on Physicochemical Properties of CdSe Aerogels (Tetranitromethane Oxidation). PXRD spectra of CdSe aerogels prepared by the use of nanoparticles from the inverse micellar route are characteristic of the cubic CdSe phase (cadmium selenide), while those of the aerogels prepared using nanoparticles from the high temperature route suggest the hexagonal, cadmoselite phase (Figure 1). Occasionally, a small peak is observed near 38° 2θ, attributable to CdO, which we ascribe to surface oxidation. The average crystallite size calculated based on the Scherrer formula shows that the CdSe crystallites within the aerogel framework are slightly larger than those for the precursor particles (Table 1); however, the core crystal structure remains unchanged upon gelation and aerogel formation.

Elemental compositions of the CdSe precursor nanoparticles and aerogels were investigated using an in situ energy dispersive spectroscopy unit coupled with scanning electron microscopy (EDS/SEM) for several individually prepared samples, and the

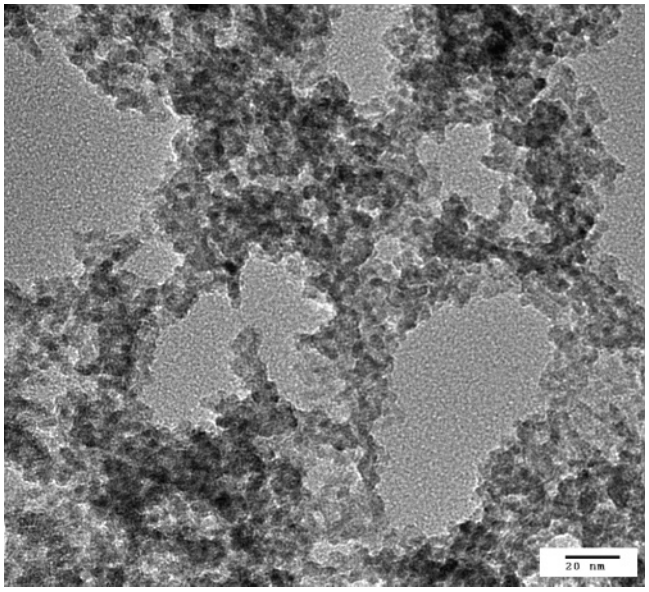

Figure 2. A transmission electron micrograph of a CdSe aerogel prepared from nanoparticles synthesized by the high temperature route. The TEM sample was prepared by dispersion in acetone, and the dark contrast observed within the network corresponds to areas of greater thickness (i.e., multiple layers of nanoparticles).

average results are presented in Table 1. Thiolate-coated CdSe nanoparticles synthesized from the inverse micellar route show three prominent peaks in the EDS spectrum corresponding to atomic ratios of Cd:Se:S of 1:1:0.5. Upon gelation with tetranitromethane and aerogel formation with supercritical CO_2, the sulfur content of the material is reduced to 9−12%. As-prepared high temperature synthesized CdSe nanoparticles show three peaks in the EDS spectrum that correspond to a Cd:Se:P ratio of 1:1:0.4. However, exchange with 11-mercaptoundecanoic acid reduced the phosphorus content of the material to less than 5%, and resulted in a sulfur content of ~20%. Upon gelation and aerogel formation, the sulfur content is reduced to 12−15% with no major change in the phosphorus content. However, the phosphorus could be completely removed (<1%) from the aerogel products, and the sulfur content reduced to ca. 6%, if the wet gels were exchanged with pyridine several times prior to aerogel formation.

Transmission electron microscopy (TEM) was employed to study the morphology of the CdSe aerogels. A TEM image of a CdSe aerogel prepared from high temperature synthesized CdSe nanoparticles shows that these materials consist of an interconnected network of nearly spherical CdSe nanoparticles (Figure 2 and Supporting Information). The CdSe aerogels prepared using nanoparticles from the inverse micellar route have a similar morphology. The presence of a meso- (2−50 nm) to macro (>50 nm)-porous structure with a wide range of pore diameters is observed throughout these materials. Primary particle size calculations using TEM images reveal an increase in particle size for aerogels compared to the precursor nanoparticles (Table 1).

The band gap values of CdSe aerogels were measured using diffuse reflectance UV−visible spectroscopy. Figure 3 shows the diffuse reflectance spectra (converted to absorption) for the as-prepared CdSe aerogels prepared from nanoparticles synthesized by inverse micellar and high temperature routes, along with the UV−visible absorption spectra of the precursor

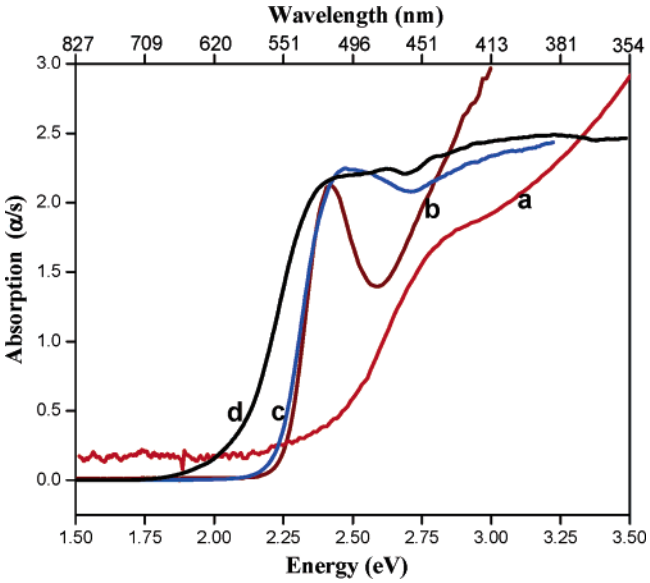

Figure 3. UV−visible absorption spectra of the CdSe precursor nanoparticles prepared by (a) inverse micellar and (b) high temperature methods, along with the diffuse reflectance UV−visible spectra (converted to absorption) of the resultant CdSe aerogels: (c) inverse micellar and (d) high temperature.

nanoparticles. Both the reverse micellar and high temperature processed aerogels show sharp optical absorption onsets. The band gap values estimated based on the absorption onset, along with the particle size calculated based on the mass approximation model, are presented in Table 1. The band gap values are smaller than the absorption onset values of the precursor nanoparticles and correlate with some degree of primary particle growth, as suggested from the PXRD and TEM studies. However, they remain considerably higher than that of bulk CdSe (716 nm, 1.74 eV).

In all cases, the particle size values calculated from the absorption onset are larger than those obtained by XRD or TEM. This may be attributed to discrepancies between the bulk dielectric constant used in the mass approximation model and the actual constant for the nanocrystals.[30] A more accurate determination of particle size can be made from the first optical transition peak. This calculation (based on the first transition peak at 510 nm) does indicate a smaller particle size (4.3 nm) relative to that from the absorption onset (5.0 nm) for high temperature prepared nanoparticles, but no further comparisons can be made since the first optical transition cannot be definitively assigned for room temperature prepared nanoparticles or any of the aerogels.

Emission properties of the nanoparticle precursors and as-prepared aerogels were investigated using photoluminescence spectroscopy (Figure 4). CdSe aerogels prepared from inverse micellar synthesized particles appear to exhibit a moderately sharp band-edge emission peak at 532 nm (Figure 4A), implying a Stokes shift of approximately 0.09 eV (Supporting Information), in the normal range reported for CdSe nanoparticles.[31] This is transposed over a rising baseline that we attribute to

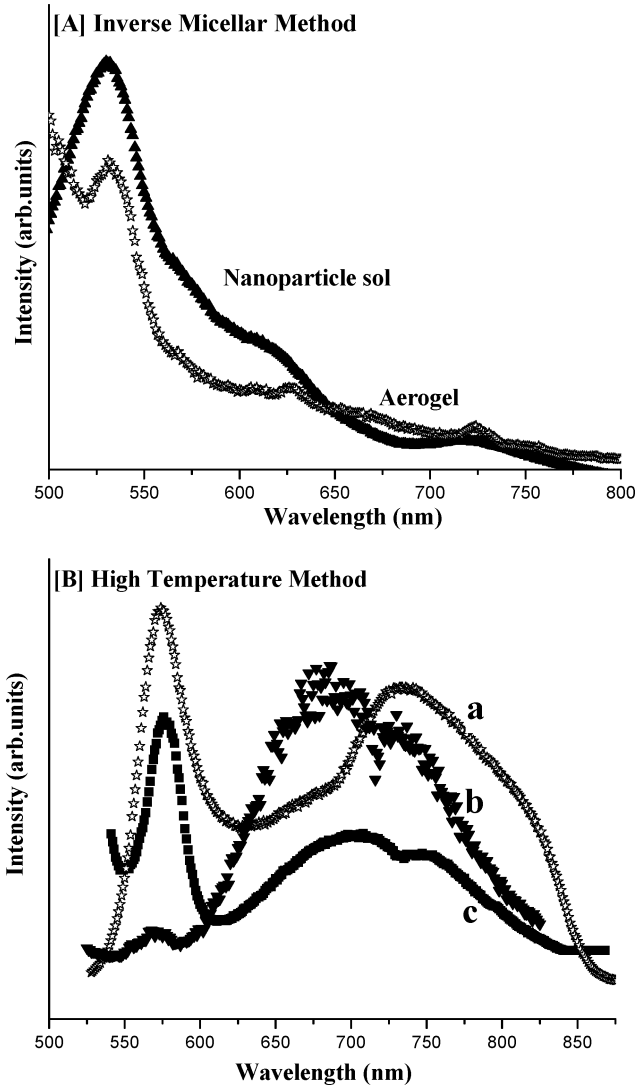

Figure 4. Photoluminescence (PL) spectra of the (A) CdSe nanoparticles prepared by the inverse micellar method and resultant aerogels. (B) CdSe nanoparticle sol prepared by the high temperature method (a), resultant aerogels (b), and aerogel resulting from gels that were exchanged with pyridine for 4−5 days before the supercritical drying (c). The data were acquired using an excitation wavelength of 480 nm.

scattering, pronounced here because of the inherently weak emission of low temperature prepared samples. These features and their relative intensities are similar to those observed in the nanoparticle precursors. In contrast, there is a large difference in the photoluminescence characteristics of the sol and aerogel when the particles are prepared by high temperature routes (compare Figure 4B, spectra a and b). The band-edge emission occurs at 570 nm (Stokes shift = 0.18 eV, Supporting Information) but is very weak compared to the trap state emission features: a broad double hump extending from 625 to 825 nm. The nanoparticles show a prominent band-edge luminescence peak with the most intense trap state features more red-shifted than for the aerogel, in the 700−850 nm range. However, if wet gels are exchanged with pyridine several times prior to supercritical drying, intensity within the band-edge feature can be recovered in the resultant aerogel, as seen in Figure 4B, spectrum c. Varying the excitation wavelength from 450 to 515 nm had no effect on the spectroscopic characteristics of high temperature prepared materials, but resulted in some

(29) Borchert, H.; Shevchenko, E. V.; Robert, A.; Mekis, I.; Kornowski, A.; Grubel, G.; Weller, H. *Langmuir* **2005**, *21*, 1931−1936.
(30) Pejova, B.; Tanuševski, A.; Grozdanov, I. *J. Solid State Chem.* **2004**, *177*, 4785−4799.
(31) Chen, X.; Samia, A. C. S.; Lou, Y.; Burda, C. *J. Am. Chem. Soc.* **2005**, *127*, 4372−4375.

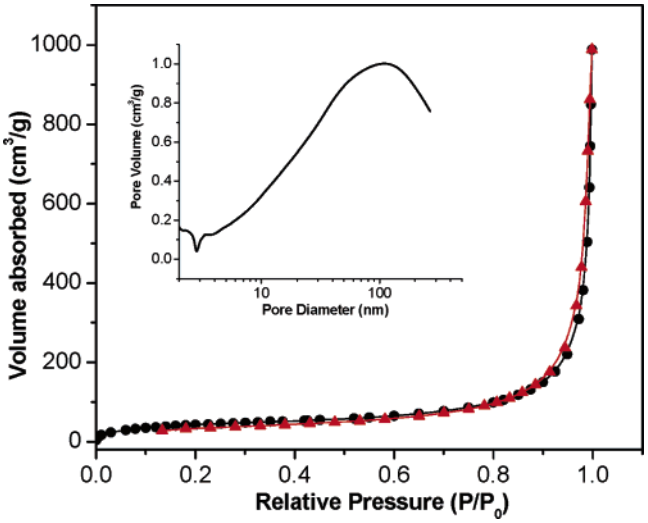

Figure 5. Nitrogen adsorption (filled circles)/desorption (filled triangles) isotherms of a CdSe aerogel synthesized from high temperature prepared nanoparticles. The inset shows the corresponding BJH modeled pore size distribution. The aerogel samples were degassed at 100 °C for 72 h before the analysis.

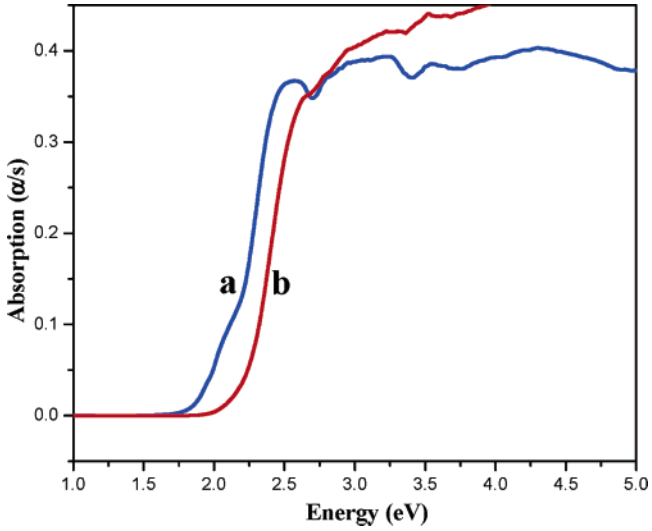

Figure 6. Diffuse reflectance UV−visible spectra of CdSe aerogels produced from inverse micellar prepared nanoparticles using (a) 3% H_2O_2 as the oxidizing agent for the gelation and (b) 3% H_2O_2 as the oxidizing agent for the gelation followed by treatment of the wet gel with 0.2 mL of 0.1 M HCl before the supercritical drying.

shift of the positions of the broad features (600−750 nm) of the inverse micellar materials and subtle changes in their shape.

The surface areas of CdSe aerogels were obtained by applying the BET model to nitrogen adsorption/desorption isotherms acquired on samples degassed at 100 °C. The average pore diameter and cumulative pore volumes were calculated using the BJH model. Figure 5 shows a typical isotherm obtained for CdSe aerogels synthesized from high temperature prepared nanoparticles along with the BJH modeled pore size distribution. BET surface areas, BJH average pore diameters, and cumulative pore volumes obtained for CdSe aerogels synthesized from both inverse micellar prepared and high temperature prepared nanoparticles are presented in Table 1. For the sake of making a direct comparison to a "traditional" aerogel, the equivalent silica surface area, assuming the mass is composed of silica instead of CdSe, is computed as well.

The adsorption/desorption isotherms obtained for the CdSe aerogels are similar in shape, regardless of the methodology used to synthesize the primary nanoparticles, and resemble a type IV curve with a sharp upturn in the high relative pressure region giving some resemblance to a type II curve.[32,33] The nitrogen desorption branch falls slightly below the adsorption branch, as a result of desorption of residual He gas (used to determine the free space value of the sample holder prior to nitrogen introduction) during the data acquisition. Hence, we report the pore diameters and cumulative pore volume from the adsorption branch. The hysteresis loops of the adsorption/desorption isotherms have a combination of H1 and H3 character that corresponds to cylindrical and slit shape pore geometries, respectively,[33] and the BJH modeled pore size distribution analysis (Figure 5, inset) shows a broad range of pores extending from 2 to 300 nm for both types of aerogels. However, the aerogels prepared from inverse micellar synthesized nanoparticles exhibit higher BET surface areas and generally greater average pore diameters and cumulative pore volumes than the aerogels prepared from high temperature synthesized nanoparticles (Table 1). In all cases, the number averaged pore diameter is in the 16−29 nm range (Table 1) as determined by the BJH model. The maximum in the distribution in the inset to Figure 5, corresponding to a pore diameter of 100 nm, is a consequence of the fact that macropores adsorb a larger volume of molecules.

With respect to the structure, composition, optical properties, and porosity characteristics, photooxidized CdSe gels and aerogels were nearly identical to the gels and aerogels obtained using tetranitromethane. Hence, for these two oxidants, the properties of the resultant aerogels are largely a function of the characteristics of the precursor nanoparticles.

Effect of Oxidant on Properties of Aerogels; H_2O_2 Oxidation of 4-Fluorobenzenethiolate-Capped CdSe Nanoparticles Prepared By The Inverse Micellar Route. The most obvious difference observed when H_2O_2 is used as an oxidant for CdSe gel preparation is the gradual change in color of the sol from red−orange to bright yellow during the course of gelation, a color that is maintained throughout the transformation to the aerogel. This color change is reflected in a red shift in the optical absorption edge of the as-prepared aerogel from 577 nm (obtained using tetranitromethane) to 589 nm (2.10 eV), along with a broad shoulder at 662 nm (1.87 eV, Figure 6a). As for gels prepared using other oxidants, the EDS spectra of CdSe aerogels prepared by H_2O_2 oxidation of the precursor nanoparticles show only three prominent peaks, and these correspond to a ratio of 1:0.9:0.28 for Cd:Se:S. However, the BET surface area of the CdSe aerogel prepared by H_2O_2 oxidation was considerably larger (224 m^2/g) than the values obtained for tetranitromethane and photooxidized gels and aerogels, with a BJH average adsorption pore diameter of 22 nm. Interestingly, while the PXRD spectra of wet gels are essentially identical to those of the precursor nanoparticles, the corresponding aerogels prepared by H_2O_2 oxidation contain crystalline $CdCO_3$ (crystallite size ∼ 35−40 nm) as an impurity along with the CdSe aerogel network (Figure 7).

Treatment of the yellow colored wet gel (oxidized with 3% H_2O_2) with 0.1 M HCl for 24 h resulted in a color change back

(32) Webb, P. A.; Orr, C. *Analytical Methods in Fine Particle Technology*; Micromeritics: Norcross, GA, 1997.
(33) Gregg, S. J.; Sing, K. S. W. *Adsorption, Surface Area and Porosity*, 2nd ed.; Academic: New York, 1982.

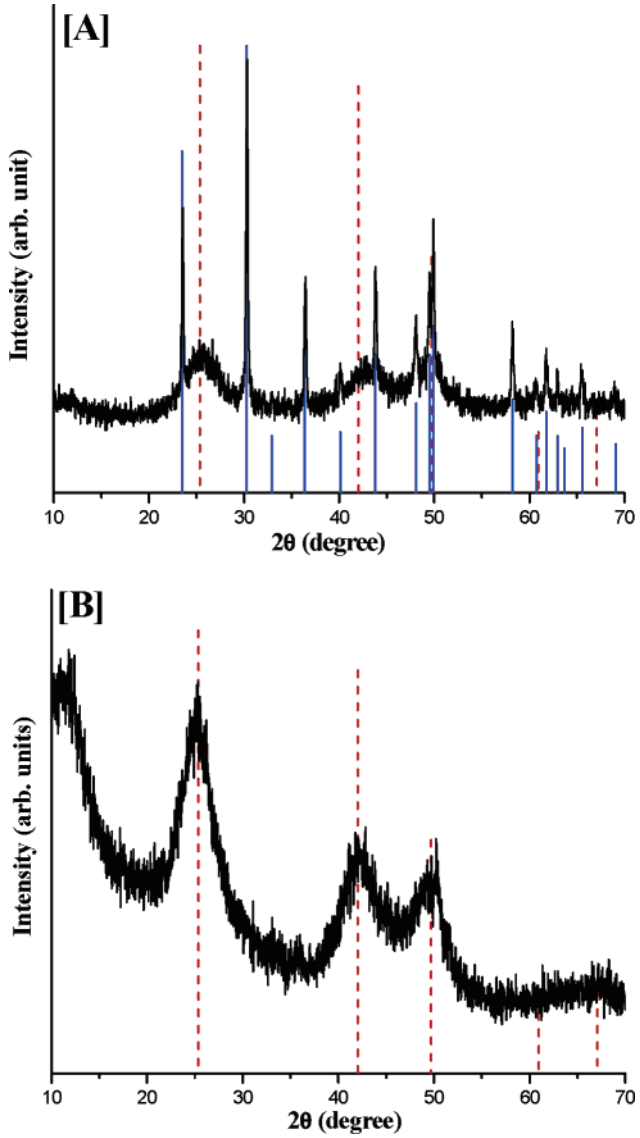

Figure 7. Powder X-ray diffraction patterns of CdSe aerogels produced from inverse micellar prepared nanoparticles using (A) 3% H_2O_2 as the oxidizing agent for the gelation and (B) 3% H_2O_2 as the oxidizing agent for the gelation followed by treatment of the wet gel with 0.2 mL of 0.1 M HCl before the supercritical drying. The ICDD-PDF overlays of cubic CdSe (PDF # 19-0191, dotted lines) and cubic $CdCO_3$ (PDF # 14-0143, solid lines) are shown as vertical lines.

to red and a remarkable decrease in the amount of $CdCO_3$ impurity in the corresponding aerogel, as probed by PXRD. The $CdCO_3$ impurity can be completely eliminated by treatment of the wet gel 2−3 times with 0.2 mL of 0.1 M HCl over 6−7 days before the supercritical drying step (Figure 7B). The color change and carbonate formation in the aerogel is not observed with tetranitromethane oxidized or photooxidized CdSe gels or with CdS, ZnS, or PbS gels treated with 3% H_2O_2.[24,25] The CdSe aerogel prepared after treating the CdSe gel (oxidized by H_2O_2) with 0.2 mL of 0.1 M HCl for 6−7 days shows a sharp absorption onset at 562 nm (2.2 eV, Figure 6b) similar to results obtained using tetranitromethane (Figure 3, spectrum c) and photooxidation, but a significantly lower BET surface area (90 m^2/g) relative to aerogels prepared without the HCl treatment, or by the use of other oxidants. Additionally, the BJH average adsorption pore diameter has increased from 22 (no HCl treatment) to 26 nm.

Discussion

CdSe gels were successfully prepared from room temperature synthesized and high temperature synthesized nanoparticles by oxidative removal of the thiolate groups from the nanoparticle surface. Three different oxidants were explored for the oxidation of thiolate groups: tetranitromethane, H_2O_2, and photooxidation in air using ambient fluorescent lighting. As the resulting disulfide and sulfonates are removed into the solution, nanoparticles aggregate to form a wet-gel network.[27] To maintain the pore structure of the network, the material is dried supercritically, forming an aerogel. All the aerogels retained a significant quantity (10−15%) of sulfur in the product, attributed to unreacted thiolate, and the Cd:Se ratio is approximately 1:1, consistent with the CdSe formulation. Additionally, aerogels prepared from high temperature synthesized nanoparticles contain about 4% phosphorus due to residual trioctylphosphine oxide and/or tetradecylphosphonic acid from the nanoparticle synthesis.

Mechanism of Gelation as a Function of Oxidant. Initial studies were focused on the use of H_2O_2 as an oxidant, as employed by Gacoin et al.,[22,23,28,34] and in our previous work with CdS, PbS, and ZnS aerogels.[25] However, attempts to perform controlled oxidation of surface thiolate groups on inverse micellar prepared CdSe nanoparticles using 3% H_2O_2 resulted in a dramatic change in color from orange to yellow over the course of gelation. Upon supercritical drying with liquid CO_2, highly crystalline $CdCO_3$ was found as a byproduct, along with peaks corresponding to nanocrystalline CdSe, suggesting phase segregation and chemical reaction with the CO_2 had occurred. Presumably, this arises from formation of hydroxide as a byproduct of the H_2O_2 oxidation, which subsequently displaces surface selenol or selenate species exposed by thiolate ligand removal, resulting in the change in optical properties. The resulting Cd hydroxide/oxide species can subsequently insert CO_2, giving rise to carbonate formation.[35] That this is not observed for sulfides can be attributed to the fact that the bond strengths for metal sulfides evaluated here (M = Zn, Cd, Pb) are not substantially different from the corresponding oxides (ΔH M−O vs M−S ∼ 20−45 kJ/mol), whereas a relatively large difference (>100 kJ/mol) in bond energies is observed for Cd−O versus Cd−Se, with Cd−O favored, providing a large thermodynamic driving force for hydroxide substitution in the latter case.

Consistent with the idea that hydroxyl moieties play an essential role in carbonate formation, the treatment of an H_2O_2-oxidized CdSe gel 2−3 times with small amounts of a slightly acidic solution over several days returns the gels to their native orange color. Supercritical drying of the resultant materials produces CdSe aerogels without any $CdCO_3$ byproduct, presumably due the neutralization and removal of the hydroxyl moieties from the CdSe surface. However, treatment with acids results in significant condensation of the gel network, as reflected in the drastically reduced surface area in the corresponding aerogels relative to materials that were not treated with acid.

Hence, we investigated the use of chemical oxidants that do not function as oxygen transfer agents or produce OH^- during the gelation process. Gacoin and co-workers have shown that

(34) Malier, L.; Boilot, J.-P.; Gacoin, T. *J. Sol−Gel Sci. Technol.* **1998**, *13*, 61−64.
(35) Doiwa, V. A.; Tomanek, A. *Z. Anorg. Allg. Chem.* **1964**, *334*, 12−14.

benzoyl peroxide or bromine does not lead to stable gels of CdS, but rather precipitates.[28] However, they did note that CdS gelation could occur with oxygen from the ambient,[23] and we have previously shown that tetranitromethane is also an effective gelation agent,[25,26] presumably by a mechanism similar to that presented in eqs 1 and 2 for 4-fluorobenzenethiol. Unlike the case for hydroxide formation from hydrogen peroxide, the nitrite byproduct, and products from nitrite disproportionation, would not be expected to displace Se from the nanoparticle surface. Consistent with this hypothesis, CdSe aerogels were obtained without any apparent impurities when tetranitromethane was used as the oxidant.

$$\mathrm{FPhSH} + \mathrm{C(NO_2)_4} \rightarrow \mathrm{FPhSNO_2} + \mathrm{HC(NO_2)_3} \quad (1)$$

$$\mathrm{FPhSNO_2} + \mathrm{FPhSH} \rightarrow \mathrm{FPhS{-}SPhF} + \mathrm{H^+} + \mathrm{NO_2^-} \quad (2)$$

Additionally, we have found that leaving CdSe sols under ambient room lights produces gels by the photocatalytic oxidation of surface-bound thiolate ligands to disulfides.[27] Scavenging of the optically excited electron by O_2 results in oxidation of bound thiolate by the hole trapped in the valence band.[36] However, the inverse micellar CdSe nanoparticles capped with 4-fluorobenzenethiolate require a long time to gel when compared to the high temperature processed CdSe nanoparticles capped with MUA. Since electron transfer to O_2 is the rate-determining step in thiolate oxidation, the large differences in gelation rate may be a function of the ability of O_2 to gain access to the nanoparticle surface, that is, differences in thiolate binding equilibria or permeability of the thiolate monolayer to O_2 diffusion. Interestingly, despite the large differences in kinetics for gelation of photooxidized versus tetranitromethane-oxidized nanoparticles, the properties (optical absorption, luminescence, surface area, etc.) of the resultant aerogels are very similar.

Effect of Nanocrystal Quality on Aerogel Characteristics. The luminescence characteristics of nanoparticles are strongly dependent on the crystallinity of the nanoparticles and their surface characteristics. In particular, high temperature synthesized CdSe nanoparticles are reported to have higher quantum yields than inverse micellar prepared materials, due to poor crystallinity and relatively high defect densities in the latter.[28,37,38] We surmised that the quality of the individual nanoparticles would form a baseline for the resultant aerogel quality. To test this assumption, we compared aerogels prepared from inverse micellar synthesized and high temperature synthesized nanoparticles, using tetranitromethane as the oxidant in all cases.

PXRD studies show that inverse micellar prepared materials adopt the cubic CdSe polymorph, whereas high temperature prepared materials adopt the hexagonal polymorph, with the latter having slightly larger crystallite sizes. In general, the crystallite sizes of primary particles within the aerogels are only slightly larger than those for the precursor particles, reflecting a low degree of sintering during the low temperature aerogel processing.

Although sintering is minimized, the chromophore size might be expected to increase due to particle−particle interactions within the network. Optical absorption onsets show a decrease in band energies (increase in chromophore size) for CdSe aerogels prepared by the use of nanoparticles either from the inverse micellar route or the high temperature route, when compared to the precursor nanoparticle sols. However, the change is small, consistent with particle growth as reflected by PXRD and TEM studies, and quantum confinement is retained in the network, ascribed to the low dimensionality of the framework.[25,26] This low dimensionality is reflected in the surface area and pore characteristics of the aerogel.

The surface area values obtained for CdSe aerogels are quite high for a non-oxide system and approach those of an average silica aerogel[2] (600 m^2/g) when compared on a per mole basis (see Table 1, silica equivalents). The adsorption/desorption isotherms obtained for both aerogels are similar in shape and resemble a type IV curve, which is characteristic of a mesoporous (2−50 nm) material. This evidence is supported by TEM studies on aerogels, as we observed a large number of mesopores and a few macropores throughout the material. In general, aerogels from inverse micellar prepared particles exhibit higher surface areas than those from high temperature prepared particles. This may be a consequence of the difference in primary particle size or reactivity impacting the dimensionality of the aggregates. Corresponding CdSe xerogels[26] prepared by benchtop drying of wet gels have much lower surface areas and average pore diameters compared to those of aerogels, as the conventional benchtop drying leads to the compaction of the gel framework due to pore collapse during solvent evaporation. The increased density of the network is reflected in a lower degree of quantum confinement.[26]

In contrast to results obtained for CdS, the band-edge luminescence observed in inverse micellar prepared nanoparticles is retained in the as-prepared aerogel materials (530 nm). The breadth is somewhat larger for the aerogel, suggesting a wider range of chromophore sizes. For both sol and aerogel, a series of weak and broad peaks between about 550 and 750 nm are observed and attributed to mid-gap trap states associated with lattice or surface defects. Contrary to expectations, the as-prepared aerogel from high temperature synthesized nanoparticles exhibited only weak band-edge luminescence at 570 nm with dominant trap state emission peaks in the 600−800 nm region, suggesting the gelation procedure resulted in augmentation of defects. We surmised that the weak band-edge photoluminescence might also be a consequence of residual thiolate capping groups, which are known to introduce surface trap states in CdSe quantum dots, mediating electron−hole recombination.[39] This is reflected in the appearance of a broad red feature in the photoluminescence spectrum of CdSe upon capping with MUA. However, introduction of excess oxidant to remove all the thiolate functionalities results in significant compaction of the gel body and/or precipitation. Accordingly, we sought to remove the residual thiolate by a ligand exchange process at the wet-gel stage. To do so, we exchanged the solvent of a wet gel prepared from high temperature synthesized nanoparticles with pyridine, a good Lewis base that has a lower propensity to introduce sites for electron−hole recombination. Multiple

(36) Raevskaya, A. E.; Stroyuk, A. L.; Kuchmii, S. Y. *J. Nanoparticle Res.* **2004**, *6*, 149−158.
(37) Bandaranayake, R. J.; Wen, G. W.; Lin, J. Y.; Jiang, H. X.; Sorensen, C. M. *Appl. Phys. Lett.* **1995**, *67*, 831−833.
(38) Murray, C. B.; Norris, D. J.; Bawendi, M. G. *J. Am. Chem. Soc.* **1993**, *115*, 8706−8715.
(39) Jeong, S.; Achermann, M.; Nanda, J.; Ivanov, S.; Klimov, V. I.; Hollingsworth, J. A. *J. Am. Chem. Soc.* **2005**, *127*, 10126−10127.

solvent changes over several days results in complete removal of residual trioctylphosphine oxide and/or tetradecylphosphonic acid (i.e., no phosphorus is detected) and a 50% decrease in the thiolate concentration relative to non-pyridine-treated materials. The resultant aerogels exhibit a dramatic increase in band-edge luminescence and a corresponding decrease in trap state luminescence. These data suggest that post-modification of wet gels is a useful strategy for tuning the properties of chalcogenide aerogels.

Conclusions

Oxidation of thiolate-capped CdSe nanoparticles yields aggregated gels that can be transformed into aerogels by supercritical drying, maintaining the loosely connected nanoparticle network present in the wet-gel. Gelation can be achieved using tetranitromethane, hydrogen peroxide, or by photooxidation, and the wet gels are susceptible to surface exchange, impacting the resultant properties of the aerogels. Hydrogen peroxide treatment results in hydroxylated surfaces that insert CO_2 during supercritical drying to form $CdCO_3$. This can be alleviated by treatment with acidic solutions. Likewise, electron−hole recombination at thiolate trap states can be reduced by solvent exchange of residual thiolates in the wet gel with pyridine. Thus, although the nanoparticles are assembled into a 3-D connected solid, they are still able to undergo surface modification, similar to the behavior of discrete nanoparticles in solution, without destroying the gel network. Importantly, the low-dimensional nature of the nanoparticle network permits quantum confinement to be retained. The sensitivity of the CdSe aerogel properties to the nature of adherent chemical species, the capacity for redox activity, and the high surface area and interconnected pore structure suggests these materials may be useful for chemical sensing, photocatalytic, or photovoltaic applications. Specific studies to test this premise are currently underway.

Acknowledgment. We thank Professor Mercouri Kanatzidis (Michigan State University) for the use of the solid state optical band gap equipment. This work was supported by the National Science Foundation (CAREER, DMR-0094273) and the donors of the Petroleum Research Fund, administered by the American Chemical Society. Electron microscopy was acquired in the WSU Central Instrumentation Facility on a JEOL 2010F purchased under NSF Grant DMR-0216084.

Supporting Information Available: Detailed experimental procedures for the synthesis of CdSe precursor nanoparticles, gels, and aerogels; characterization techniques and sample preparation methods. Diffuse reflectance UV−visible spectra and photoluminescence spectra of CdSe aerogels prepared from nanoparticles prepared by inverse micellar and high temperature methods. TEM images of CdSe aerogels prepared from high temperature synthesized nanoparticles (TEM sample prepared without solvent). This material is available free of charge via the Internet at http://pubs.acs.org.

JA061561E